Journal of Cleaner Production 244 (2020) 118737

Contents lists available at ScienceDirect

Journal of Cleaner Production

journal homepage: www.elsevier.com/locate/jclepro

Bio-CH_4 from palm empty fruit bunch via pyrolysis-direct methanation: Full plant model and experiments with bio-oil surrogate

Hafizah Abdul Halim Yun [a, b], Sergio Ramírez-Solís [a], Valerie Dupont [a, *]

[a] School of Chemical and Process Engineering (SCAPE), University of Leeds, Leeds, LS2 9JT, UK
[b] Faculty of Engineering, Universiti Malaysia Sarawak, Sarawak, 94300, Malaysia

ARTICLE INFO

Article history:
Received 15 May 2019
Received in revised form
2 September 2019
Accepted 5 October 2019
Available online 7 October 2019

Handling editor: Jun Bi

Keywords:
Synthetic natural gas (SNG)
Biomethane
Palm empty fruit bunch (PEFB)
Pyrolysis
Methanation
Acetic acid
Nickel

ABSTRACT

A promising, cleaner alternative process of thermochemical conversion of lignocellulosic biomass to biomethane is proposed and rigorously investigated via modelling and experiments for the first time. Using a conventional nickel on calcium aluminate catalyst, operated in bench scale at 1 atm, 400 °C, and with a feed molar steam to carbon ratio of 2, the Low Temperature Steam Reforming of acetic acid, representing a single compound bio-oil surrogate, achieves a promising 81.9% fuel carbon conversion to gases with a methane yield of 15.7 wt% of the feed. This compares to 21 wt% methane yield at equilibrium, thus demonstrating encouraging first time performance and scope for future catalyst optimisation. A comprehensive Aspen Plus model is developed for the first time for an industrial plant producing biomethane from palm empty fruit bunch (50 wt% initial moisture), an under-used agro-industrial waste produced in vast amounts in South-East Asia and Sub-Saharan Africa. Dependency on external heating is completely eliminated by heat recovered from combusting 25% of the gas product. Based on the simulation results of the autothermal plant, a final gas product consisting of 99.2 wt% of CH_4 and 0.8 wt% of H_2 is predicted with a plant thermal efficiency of 80.6%, i.e., comparable to modelled efficiencies found in the literature for wood gasification to biomethane plants that generate syngas as a necessary intermediate.

1. Introduction

Biomass is considered a reliable source of energy because it is geographically abundant, and can contribute significantly to controlling environmental impacts such as global warming (Owusu and Asumadu-Sarkodie, 2016). The production of substitute natural gas also known as synthetic natural gas (SNG) from biomass (bio-SNG) is the motivation of the present study in reducing the strong dependency on conventional (fossil) natural gas because of its composition, which is mostly methane (CH_4) (Kopyscinski et al., 2010). In addition, SNG can contribute by prolonging the number of years of production left with relation to known reserves of natural gas (R/P), which on the basis of various studies, are limited to 52.8 years (R/P is sensitive to the discovery of reserves, increase or decrease of annual production) (Dudley and UK, 2016).

Palm empty fruit bunch (PEFB) is the main contributor to the palm oil derived biomass by-product, with 15.5–17.5 million tons per year. Most of the palm oil millers do not have the technology for the disposal of empty fruit bunch (EFB) (Abas et al., 2011). EFB is typically left in piles without any further application, and large amounts of it eventually undergo uncontrolled anaerobic digestion, thus generating atmospheric CH_4 emissions (Singh and Bajpai, 2012) as well as causing odour related nuisance.

Thermochemical conversion of lignocellulosic biomass (agricultural, forestry and wood residues) into CH_4 is commonly based on the gasification process, following a similar layout as gasification of solid fuel (mainly coal) (Solarte-Toro et al., 2018). The biomass feedstock undergoes the gasification, methanation, and purification. The gasification process to convert biomass into SNG, which is described by reaction EQ. 1, requires high operating temperatures (700–1000 °C) to produce CH_4, CO, CO_2, light and heavy hydrocarbons and char (Ni et al., 2006).

$$Biomass \xrightarrow{Heat} H_2 + CO + CH_4 + CO_2 + hydrocarbons\ (tars) + char \quad \text{EQ. 1}$$

Gasification suffers from low selectivity to gas products, with

* Corresponding author.
E-mail address: V.Dupont@leeds.ac.uk (V. Dupont).

https://doi.org/10.1016/j.jclepro.2019.118737

typically methane and other alkanes being produced at this stage. It is clear from the reactions ((EQ. 2) – (EQ. 4)) which represent the methanation stage that the presence of methane in the feed from the gasifier stage would adversely affect the kinetics and equilibria of the listed reactions towards methane production. Conventional processes of SNG production from wood feedstock typically feature a gas cleaning section, and then a train of catalytic methanation units with intercooling stages needed to increase conversion (Van der Meijden et al., 2010). In the gas cleaning section, tar reforming is usually required before the cleaned syngas enters the methanation stage in order to prevent catalyst poisoning by the heavy tars generated during gasification. Catalytic tar reformers are usually operated at high temperatures in the range of 710–890 °C (Phillips et al., 2007; Fendt et al., 2012). Therefore, many researchers have developed syngas cleaning with the aim of making biomass gasification technology more attractive (Göransson et al., 2011).

$$CO + 3H_2 \leftrightarrows CH_4 + H_2O, \quad \Delta H_{298K} = -206.2 \text{ kJ/mol } CH_4 \qquad \text{EQ. 2}$$

$$2CO + 2H_2 \leftrightarrows CH_4 + CO_2, \quad \Delta H_{298K} = -247.3 \text{ kJ/mol } CH_4 \qquad \text{EQ. 3}$$

$$CO_2 + 4H_2 \leftrightarrows CH_4 + 2H_2O, \quad \Delta H_{298K} = -165.0 \text{ kJ/mol } CH_4 \qquad \text{EQ. 4}$$

Moreover, several studies have been looking for a solution to reducing internal reforming tars by providing potassium inside the gasifier (Thunman and Seemann, 2017) and by using suitable bed materials with a moderate tar cracking activity (Zhang et al., 2015). The general gasification process of conversion of biomass to methane thus appears costly and complex to operate due to generation of heavy tars associated with the gasification stage. In contrast, pyrolysis converts biomass to bio-oil (light tars), gas and solid products, as in equation (EQ. 5) by thermal decomposition of biomass in the absence of oxygen at lower temperature within 350–550 °C (Bridgwater, 2012; Zhang et al., 2005). Therefore a alternative route of bio-SNG production from lignocellulosic biomass which, like pyrolysis, avoids the formation of heavy tars, would present a cleaner and less operationally complex alternative process.

$$Biomass \xrightarrow{Heat} bio-oil(light\ tars) + hydrocarbon\ gases + char \qquad \text{EQ. 5}$$

Catalytic low temperature steam reforming process (LTSR) has revealed potential benefits for glycerol conversion (White et al., 2018). The present study introduces an alternative process of conversion of lignocellulosic biomass to methane by fast pyrolysis of the solid biomass feedstock followed by direct methanation of the pyrolysis bio-oil by LTSR. This approach, in addition to avoiding the formation of heavy tars, would in theory decrease the enthalpy gap currently inherent to the gasification/CO-methanation process, resulting in smaller temperature gradients, thus less thermodynamic irreversibilities and a therefore more efficient methanation.

The present study focusses first on demonstrating experimentally the feasibility of the direct catalytic methanation (using a nickel on calcium aluminate catalyst) of acetic acid (AcOH), chosen as a single compound bio-oil surrogate feedstock. AcOH and phenol were the most abundant species measured in bio-oil mixturesderived from palm empty fruit bunch (PEFB) (Abdullah et al., 2011; Sukiran et al., 2009; Zin et al., 2012), where GC-MS analysis accounting for 75% of the detected area peaks attributed 32% and 21% to AcOH and phenol. Flowsheeting of the pretreatment and fast pyrolysis of PEFB to a realistic bio-oil mixture, and the latter's subsequent direct methanation by LTSR and purification to bio-CH_4, was then performed on Aspen Plus V10 to show comparable thermal plant efficiencies as the wood gasification-methanation of CO/CO_2 route.

2. Methodology and materials

2.1. Catalytic experiments of direct methanation of acetic acid

The instrumented set-up is illustrated in Fig. 1. For each run, the stainless steel-made reactor was loaded with 4 g of NiO/Ca–Al_2O_3 catalyst provided by TST ltd, with particle sizes ranging from 250 to 355 μm. The reactor temperatures were controlled by an electrical tubular furnace enclosing the reactor and monitored using a thermocouple type K placed strategically close to the catalyst bed for increasing reliability on the temperature measurements. The activation of the fresh NiO-containing catalyst to metallic Ni, performed prior to feeding AcOH and water, was achieved by reduction at 600 °C under a 200 cm^3/min feed gaseous mixture composed of 95 vol% N_2/5 vol% H_2 until return of steady state. The tubular reactor was purged and cooled using a high N_2 flowrate. The temperature was then reduced until it reached the optimal range selected to conduct the LTSR experiments, namely between 350 and 450 °C. The methanation trials were conducted using feed molar steam/carbon ratios (S/C) between 1 and 3 with a N_2 carrier flow rate of 18 cm^3/min which facilitated elemental balances. AcOH and water, were pumped using syringe pumps at flow rates of 0.978 cm^3/h (equivalent to a carbon element input of 9.5×10^{-6} mol/s) and between 0.616 and 1.849 cm^3/h (varying as a function of the desired S/C), at standard temperature and pressure (STP), respectively. Volatile and non-volatile compounds were separated from the output stream by condensation, and the liquid condensate was collected for further analysis, which showed negligible presence of

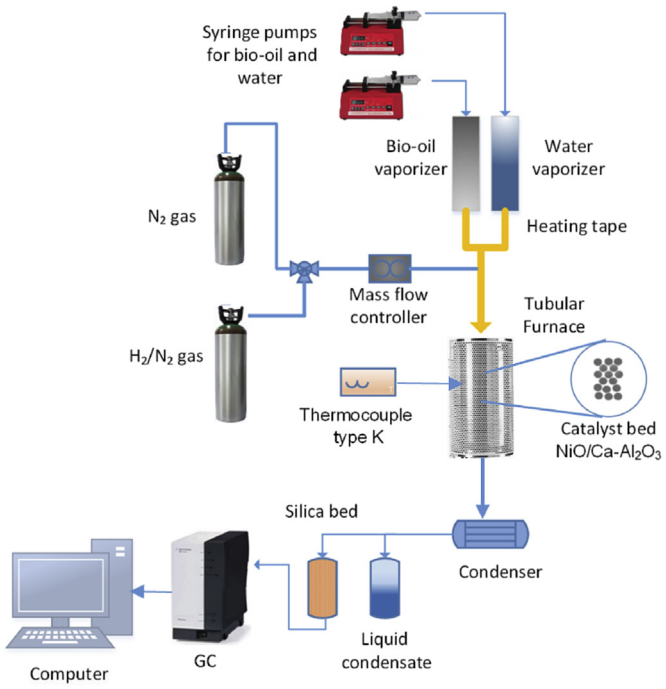

Fig. 1. Schematic diagram of the experimental set-up used for bio-oil surrogate acetic acid conversion into CH_4 production via LTSR.

carbon. Subsequently, a bed of silica gel removed residual moisture of the gas after the condensation stage. Then, the dry gas was analysed by means of a Variant CP 4900 micro GC equipped with two columns (molecular sieve 5A and Pora Plot Q) that allowed quantifying CO_2, hydrocarbons (C_2H_4, C_2H_6, C_3H_6, C_3H_8, CH_4), O_2, CO, H_2 and N_2 using argon as GC carrier gas.

2.2. Modelling and simulation

Aspen Plus (V10) has proven its capability in modelling whole plant simulations such as bio-methane production via biomass gasification processes (Van der Meijden et al., 2010; Fendt et al., 2012; Vitasari et al., 2011; Begum et al., 2013; Tremel et al., 2013) and fast pyrolysis of biomass for bio-oil production processes (Peters et al., 2014; Ward et al., 2014; Onarheim et al., 2014; Sharma et al., 2015). The properties of PEFB, which is used in this study as lignocellulosic biomass, are not included in the databank of chemical compounds of the modelling software, and thus, were defined manually into the Aspen Plus software using thermodynamic properties such as enthalpies and densities calculated by means of empirical correlations. Based on the chemical composition of bio-oils, the Peng-Robinson (Peng-Rob) property method was used, as this model is adequate for nonpolar and mildly polar compounds such as oxygenated hydrocarbons. In addition, Peng-Rob was utilized because it is also suitable for hydrocarbon-processing, gas-processing, petrochemical and refinery applications. For the CH_4 purification unit placed in the proposed bio-methane production plant (hifh pressure water scrubbing or HPWS), which works under the physical absorption/desorption principle, the Non-Random-Two-Liquid (NRTL) method was selected as the behaviour of the gases dissolved in liquid (water) was described by Henry's law. This method has been previously utilized to simulate technologies for synthetic biogas upgrading by HPWS (Cozma et al., 2015).

2.3. Model development

The methane production, which is a steady state model, consists of four main process units: 1) biomass pre-treatment, 2) fast pyrolysis of the dried and chopped biomass particles, 3) direct methanation of the bio-oil pyrolysis product via LTSR, and 4) upgrading of the reformate to high-purity methane "bio-SNG". Fig. 2 presents a flowchart that displays the main units, inputs and outputs of the conversion plant before heat integration. The biomass plant was modelled based on 3000 kg/hr of PEFB feedstock that had a realistic high moisture content of 50 wt %, which represented a huge energetic but unavoidable burden on the plant. PEFB was considered to have an initial size of 25 mm (Ward et al., 2014; Onarheim et al., 2014).

In the methanation unit, modelled under isothermal conditions based on (Yun and Dupont, 2015), the pyrolysis-derived bio-oil was converted mainly to CH_4 and CO_2. A CH_4-enriched stream was produced by using high-pressure water scrubbing technology (HPWS), validated by data from (Cozma et al., 2015). The details of the different configurations and approaches proposed to modelling each processing unit are described under the results and discussion sections.

3. Results and discussion

3.1. Experimental: Methanation of AcOH as bio-oil surrogate in a packed bed reactor

Direct methanation of acetic acid experiments, which were carried out in a packed bed reactor, were initially conducted to determine the optimal conditions to maximize the production of CH_4 and to assess the basic technological feasibility of the proposed core process of the bio-SNG plant. Temperatures of 350–450 °C and feed molar steam to carbon ratios (S/C) of 2–3, this range of S/C was successfully modelled and used in previous research works of methanation, to drive forward LTSR reactions (Yun and Dupont, 2015; Li et al., 2013). In the following sections, results of the effect of both temperature and S/C in the methanation performance are presented and discussed. The equations used to determine conversion, selectivity, yield and yield efficiencies are detailed in the supplementary data.

3.1.1. Effect of temperature in the LTSR of acetic acid

Fig. 3-c shows the effect of temperature (350–450 °C) on the outlet gas production (in mol/s) and Table 1 lists the outputs in the methanation process performed with S/C ratio of 2 and near atmospheric pressure. With just 29.4%, at 350 °C the conversion to

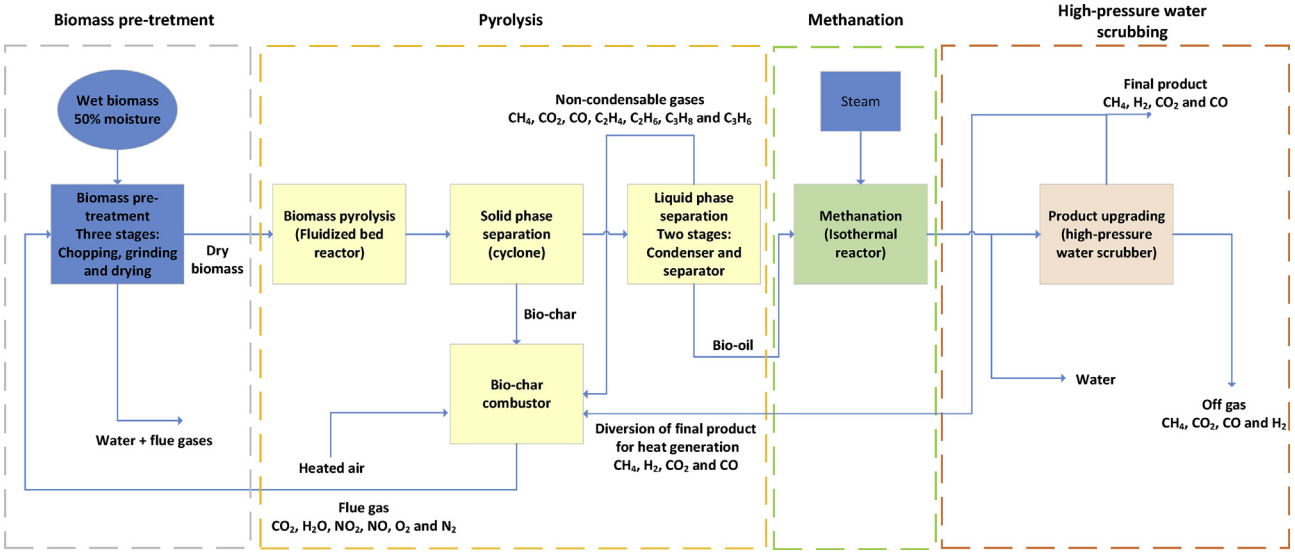

Fig. 2. Block diagram of the transformation of wet PEFB to high-purity bio-SNG via fast pyrolysis, low-temperature steam reforming (LTSR) of bio-oil, and high-pressure water scrubbing for CO_2 removal. (not featuring recycle stream, heat integration or steam generation).

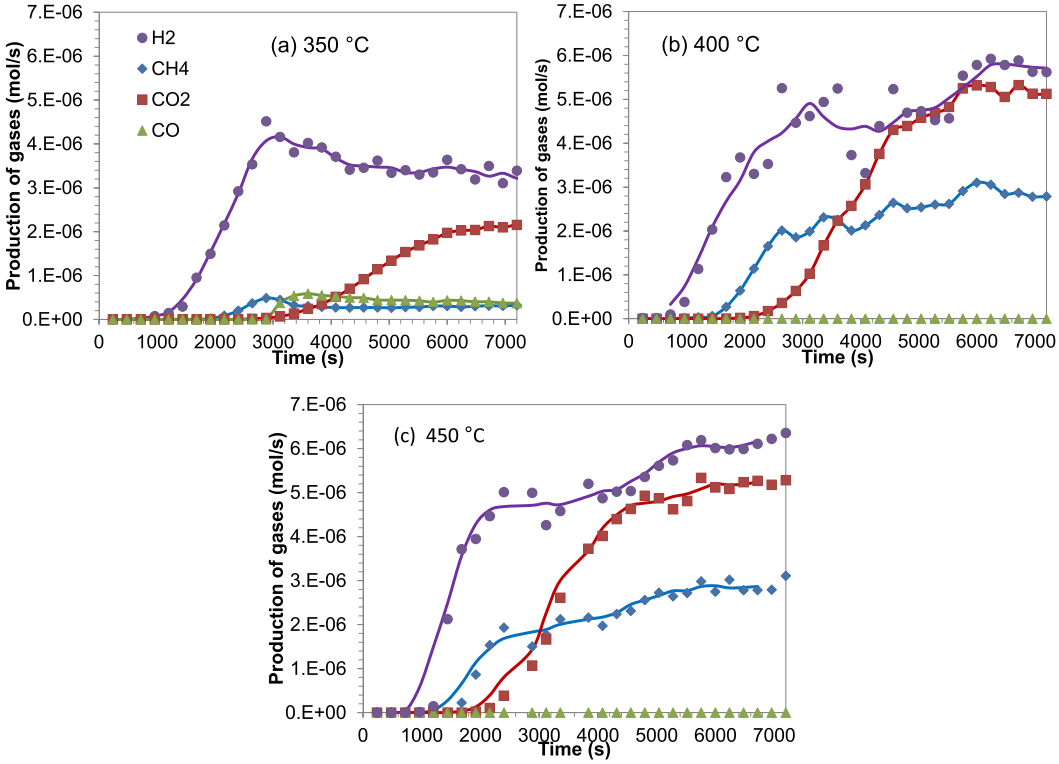

Fig. 3. Production of gases (H_2, CH_4, CO_2, and CO) at (a) 350 °C, (b) 400 °C and (c) 450 °C. The value of steam to carbon ratio of 2 was used at atmospheric pressure (feed carbon of 9.5×10^{-6} mol/s).

Table 1
The effect of reaction temperature towards CH_4 production from AcOH at constant S/C of 2 using 4 g of NiO/Ca−Al_2O_3 catalyst, post reduction under H_2.

Temperature, °C	350 °C	400 °C	450 °C
Fuel conversion to gases, %	29.4	81.9	78.6
CH_4 yield, wt.% of AcOH feed (Experimental)	1.7	15.7	14.6
CH_4 yield, wt.% of AcOH feed (Equilibrium)	23.6	21.0	17.2
CH_4 yield efficiency, % (Experimental/Equilibrium)	7.3	74.8	86.1
% Selectivity to C-products in the gas			
i. CH_4	11.0	35.8	35.2
ii. CO_2	74.8	64.2	64.8
iii. CO	14.2	0.0	0.0
% Selectivity to H-products in the gas			
i. CH_4	8.5	34.4	31.5
ii. H_2	91.5	65.6	68.5

the carbon containing gases CO, CO_2 and CH_4 ('C-gases') of the bio-oil surrogate was very low, but a substantial increase to 81.9% was obtained just 50 °C higher at 400 °C Fig. 3-b, proving the high sensitivity to temperature of LTSR for methane production. At 450 °C Figs. 2c), 78.6% feedstock conversion to C-gases was measured, comparable to that at 400 °C and with a similar selectivity to CH_4. Therefore, temperatures above 350 °C and up to 400 °C were conducive to obtaining higher fuel conversions to methane. These performance findings are consistent with those reported in (Gao et al., 2013; Garbarino et al., 2014; Abu Bakar et al., 2011).

From Table 1, the highest value of CH_4 yield was obtained at 400 °C with 15.7 wt% of the AcOH feed. In the same manner than conversion, yield efficiency increased as a function of the temperature in the range studied. As expected, kinetics are favoured at temperatures above 350 °C, and thus, it promoted a methanation yield closer to its equilibrium equivalent. The experimental results shown in Table 1 confirm that the best CH_4 yield efficiency was produced at conditions close to the equilibrium at 450 °C.

3.1.2. *Effect of feed molar steam to carbon ratio (S/C) on the conversion to CH_4 of bio-oil surrogate acetic acid*

The results displayed in panels (a)–(c) of Fig. 4 reveal that excessive water (S/C = 3) supplied into the packed bed reactor resulted in a slower reaction rate for CH_4 production. This marked delay was attributed to the presence of the water gas shift reaction (EQ. 6), which occurs as water is supplied in the process, and thus provides a competing route of the CO intermediate conversion to CO_2 rather than CH_4 with concurrent production of the H_2 by-product.

$$CO + H_2O \leftrightarrows H_2 + CO_2, \quad \Delta H_{298K} = -41 \text{ kJ/mol CO} \qquad \text{EQ. 6}$$

In terms of catalytic performance of Ni/Ca−Al_2O_3 catalyst at S/C ratios of 1–3 and 400 °C, results are summarized in Table 2.

CH_4 yield of 15.7 wt% of feed AcOH and CH_4 selectivity of 35.8% respectively at S/C of 2 confirm this ratio and temperature as the best conditions of these trials. Table 2 shows that a lower CH_4 yield was obtained at S/C of 1. While the reaction of direct methanation of oxygenated hydrocarbons (or LTSR) takes the generalised form given in (EQ. 7), in the unusual case of AcOH ($C_2H_4O_2$), the stoichiometric coefficient for the water reactant for 1 mol of AcOH feed is 0, generating one mol of CO_2 and one mol of CH_4. Thus in theory, S/C should not affect the equilibrium of LTSR of AcOH if EQ.7 was the only reaction. However, equilibrium calculations using the minimisation of Gibbs Energy method result in a large yield of solid carbon at S/C of 0, decreasing at S/C of 1 and disappearing at S/C of 2, and moles of H_2 by-product overtaking CH_4 at S/C of 3, just as in the present experiments. The latter indicates large sensitivity to feed molar steam to carbon ratio of the LTSR process for methane production .

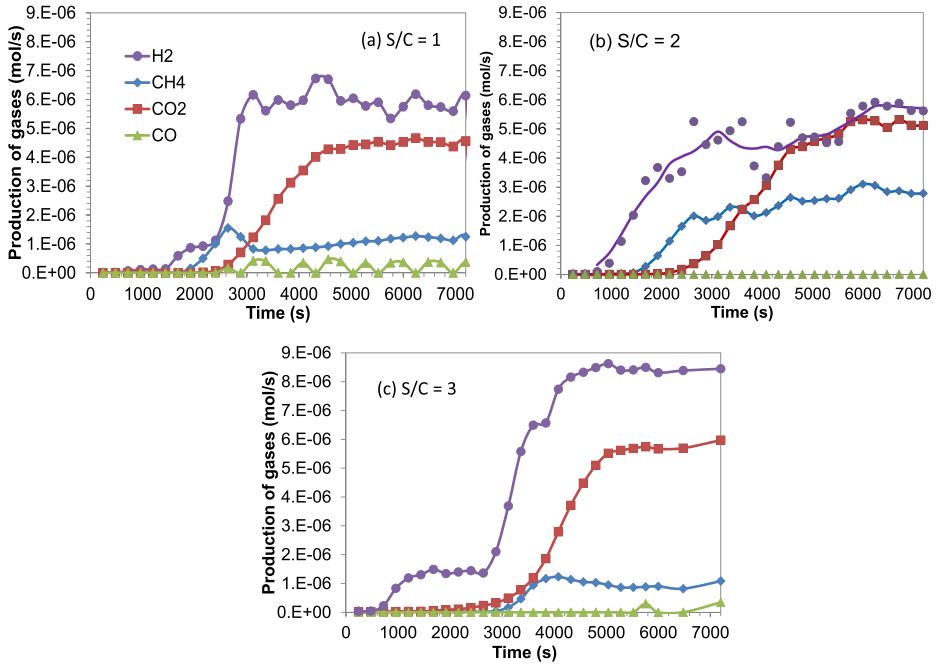

Fig. 4. Production of gases from AcOH (CH_4, CO_2, CO and H_2) at S/C of (a) 1, (b) 2 and (c) 3. The operating conditions were 400 °C and atmospheric pressure for C-feed of 9.5×10^{-6} mol/s.

Table 2
The effect of steam to carbon ratio on CH_4 production from acetic acid (AcOH) using 4 g of Ni/Ca−Al_2O_3 catalyst; experiments performed at 400 °C and 1 atm.

Steam to carbon ratio, S/C	1.0	2.0	3.0
Fuel conversion to gases, %	61.8	81.9	72.2
CH_4 yield, wt.% of AcOH (Experimental)	6.5	15.7	5.3
CH_4 yield, wt.% of AcOH (Equilibrium)	19.0	21.0	19.2
CH_4 yield efficiency (Exp./Equil.)	34.2	74.8	27.4
Selectivity to carbon (%):			
i. CH_4	19.7	35.8	13.6
ii. CO_2	76.5	64.2	84.5
iii. CO	3.9	0.0	1.9
Selectivity to hydrogen (%):			
i. CH_4	16.5	34.4	9.8
ii. H_2	83.5	65.6	90.2

$$C_nH_mO_k + \left(n - \frac{1}{4}m - \frac{1}{2}k\right)H_2O \rightarrow \left(\frac{1}{2}n - \frac{1}{8}m + \frac{1}{4}k\right)CO_2 + \left(\frac{1}{2}n + \frac{1}{8}m - \frac{1}{4}k\right)CH_4 \quad \text{EQ. 7}$$

Optimal conditions for the effective production of methane from acetic acid over a Ni/Ca−Al_2O_3 catalyst were therefore at 400 °C and S/C of 2, which brought the experimental yield of CH_4 to 75% of the equilibrium value. This experimental study confirmed (i) the feasibility of producing methane directly from bio-oil surrogate acetic acid (via 'direct methanation'), the strong dependence on (ii) temperature and (iii) feed molar steam to carbon ratio which can tip the balance of products towards either solid carbon or hydrogen.

3.2. Characteristics and pre-treatment of biomass in the plant model

PEFB was defined as a non-conventional component in Aspen Plus. It must be highlighted that the PEFB's elemental composition is represented by empirical factors in the program, whereas enthalpies and densities are determined through empirical correlations. Thus, the PEFB properties defined in the simulation environment were chosen on the basis of experimental data reported in (Abdullah et al., 2007) and the results of the proximate and ultimate analysis are given in Supplementary Data (Table A2.3). The modelled bio-oil mixture (compounds and their mass fractions) was constructed by firstly using García-Pérez et al.'s methodology (Garcia-Perez et al., 2007) on the DTG data of PEFB oil (Figure A2.1), which allowed to identify 6 macrofamilies of unspecified compounds of increasing volatility, and then to distribute their mass fractions over a small number of specified model compounds of boiling point range and chemical structure close to those identified by GC-MS (Zin et al., 2012), while preserving the overall elemental balance of the mixture (procedure implemented using Solver in Excel). The latter approach represents a valuable and novel way of better representing real bio oils by designing mixtures of model compounds, which, together, present the same volatility and elemental make-up via a rigorous methodolgy.

As mentioned in section 2.3, in the pre-treatment facility of the plant model, PEFB was assumed to have an initial size of 25 mm (Yang et al., 2006; Ruengvilairat et al., 2012). Subsequently, fibre size was reduced to 5 mm by means of a crusher. Based on the limited number of studies available in the literature for the PEFB crushing process, it was found that approximately 90 kW [61] was the power required for crushing 3000 kg/h of PEFB. Then, the 5 mm fibres were passed through a dryer to lower the excess of water to ~8 wt % as this would permit to reduce the water content in the oil mixture produced after the pyrolysis facility. Lastly, the finely crushed dried fibres, were further ground to be 1 mm as in ref (Mohammed et al., 2012), to be fed into the fluidized bed fast pyrolysis reactor.

Moisture was fed into the process as a conventional component, and 50 wt % moisture was suggested as in typical fresh PEFB (Zhang et al., 2015; Machinery, 2016).

The biomass-to-fuel efficiency and the thermal efficiency values have a strong dependency on the selection of appropriate lower

heating value (LHV) for the feedstock and product. In Table 3, a review of the LVH values of dry wood obtained from refs (Van der Meijden et al., 2010; Fendt et al., 2012; Tremel et al., 2013; Gassner and Maréchal, 2009; Duret et al., 2005) compared with LHV predicted from EQ. 8 to EQ. 10 is shown. LHV from works reported in the literature and their equivalents calculated using the elemental compositions stated in the same refs are also presented in Table 3. The LHV for wood on a dry basis were similar to those using expressions EQ. 8 to EQ. 10. The LHV of 16.83 MJ/kg calculated in this work for PEFB (dry basis) and based on ultimate analysis, was used for the plant model as it was within the range of LHV for PEFB reported in the literature from 17.02 to 20.34 MJ/kg (Kerdsuwan and Laohalidanond, 2011; Yang et al., 2006; Ruengvilairat et al., 2012; Mohammed et al., 2012; Sukiran et al., 2011; Shariff et al., 2014).

In terms of both higher (HHV) and lower (LHV) heating values for dry biomass, estimations were conducted using Channiwala and Parikh's correlation EQ. 8 (Channiwala and Parikh, 2002) and equation EQ. 9, respectively. Considering that raw PEFB with 50 wt % moisture content was utilized in this study, the LHV value on wet basis ($LHV_{biomass,\ wet}$) employed to determine thermal efficiency and energy consumption for methane production was predicted on the basis of the mathematical expression EQ. 10 (Lind et al., 2012).

$$HHV_{biomass,\ dry\ (Channiwala\ \&\ Parikh)} = 0.3491C_C + 1.1783c_H + 0.1005C_S + 0.1034C_O + 0.0151C_N + 0.0211C_A \quad \text{EQ. 8}$$

$$LHV_{biomass,\ dry}\ (Lind) = HHV_{biomass,\ dry} - H_{evap}\left(W_H x\frac{M_{water}}{M_H} + \frac{f_M}{1-f_M}\right) \quad \text{EQ. 9}$$

$$LHV_{biomass,\ wet}(Lind) = LHV_{biomass,\ dry} x\left(\frac{M_{dry}}{M_{wet}}\right) = LHV_{biomass,\ dry} x(1-f_M) \quad \text{EQ. 10}$$

A directly heated single-pass rotary dryer was selected for the drying of the PEFB because it is the most common type of dryer used for biomass according to (Amos, 1998). The drying operation is performed when the hottest gases are contacted with the wettest biomass inside a rotating drum (wet biomass and hot flue gas flow co-currently through the dryer). The continuous rotation of the drum promotes a homogeneous transfer of heat and mass due to its lifting the solids in the dryer causing them to tumble through the hot gas. Most dryers are not designed to completely dry the biomass in order to avoid over-drying of biomass, which might cause ignition and fire hazards (Amos, 1998; Fagernäs et al., 2010).

This is why the moisture content in the PEFB pyrolyzer feed should be between 8 and 10 wt % (Ward et al., 2014; Onarheim et al., 2014). Consequently, the 7.95 wt% of moisture still present in the biomass (Abdullah et al., 2011) was listed as a non-conventional component, indicating a 'dry' PEFB, whilst the remaining 1380.75 kg/h of water was specified as a conventional component. Thus, the energy required for drying up the wet PEFB was calculated by using Aspen Plus without considering the moisture content in 'dry' PEFB that as a non-conventional component, did not participate in any phase or chemical equilibrium calculations in the drying process.

Flue gases from the combustion of bio-char pyrolysis by-product were used in this study as the medium for drying the moist PEFB (FLUE-G1). It has been reported that the outlet temperature from rotary dryers can vary from 71 to 110 °C (Amos, 1998). Thus, the amount of energy needed for the PEFB drying process by using flue gases from the bio-char combustion was determined by maintaining the outlet temperature of the dryer at 110 °C.

The drying process was modelled in Aspen Plus using an RYIELD block while a separator block was chosen to split the water from the dry PEFB by phase solid/vapour separation. Then, the dry PEFB finely ground through a crusher into particles of 1 mm was fed into

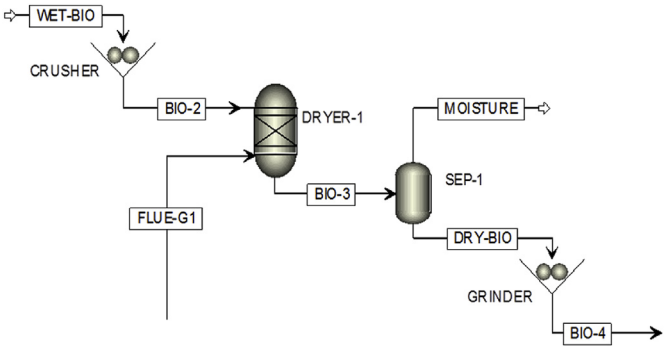

Fig. 5. Simplified flowsheet for the pre-treatment of biomass (drying and sizing).

Table 3
Elemental analysis and heating values (HHV and LHV) of lignocellulosic biomass feedstocks for CH_4 production, by using Channiwala and Parikh's expression (EQ. 8), and Lind's expression (equation EQ. 10). mf = moisture free.

Biomass	Our work, based on (Abdullah et al., 2007)	Fendt et al. (2012) (Fendt et al., 2012)	Tremel et al. (2013) (Tremel et al., 2013)	Meijden (2010) (Van der Meijden et al., 2010)	Gassner (2009) (Gassner and Maréchal, 2009)	Duret et al. (2005) (Duret et al., 2005)
	PEFB	Beech wood	Spruce wood	Wood	Wood	Wood
Moisture, wt.%	50	20	25	15	50	0
Elemental analysis, mf wt. %						
i. C	49.07	47.97	49.80	50.19	50.60	47.42
ii. H	6.48	5.78	6.30	6.04	5.70	6.25
iii. O	38.29	45.39	43.20	42.37	42.50	46.33
iv. N	0.70	0.22	0.13	0.30	0.20	0
v. S	0.10	0.03	0	0.06	0	0
vi. Cl	0	0	0	0.05	0	0
vii. Ash	5.36	0.61	0.57	1.00	1.00	0
Heating values, MJ/kg						
$HHV_{biomass,dry}$ EQ.8	20.69	18.85	20.33	20.24	19.96	19.13
$LHV_{dry\ biomass}$ (Lind + EQ.8)	16.83	16.97	18.13	18.48	16.27	17.75
$LHV_{dry\ biomass}$ (journal + Lind)	17.02–20.34	16.53	19.40	18.80	18.60	18.20

the pyrolysis facility (see Figure 5). In the literature, there is a limited number of studies for PEFB crushing process, and therefore it was assumed that the power requirement for crushing PEFB was the same as that for wood. This is because the power requirements for crushing both wood and PEFB into the same size (10–30 mm) with the same feedstock capacity (3–5 tonne biomass/h) were found to be the same, i.e. 45 kW according to (Dincer and Acar, 2015). As a result, it was assumed that the electricity consumption for finely crushing PEFB was the same as for wood, resulting in 140 kWh on dry basis. Thus, the energy demand for grinding 1619.25 kg/h of dry PEFB into particles of 1 mm was estimated to be 227 kWh.

3.3. Bio-oil production via fast pyrolysis

In this study, the pre-treated biomass (dry PEFB) was fed into a fluidized bed pyrolyzer at 500 °C and atmospheric pressure to maximize the bio-oil yield, based on (Sharma et al., 2015). Attributable to lack of reaction mechanism data or kinetic data for this process, a RYIELD block was used to simulate the pyrolysis. Product yields through the pyrolysis process were defined based on literature data. For modelling this fluidized bed pyrolyzer, data were taken from the cited literature as follows: overall product yield from (Abdullah et al., 2007), non-condensable gases from (Abdullah et al., 2007), char from (Sukiran et al., 2011) and composition of bio-oil from (Pimenidou and Dupont, 2012) (listed in Supplementary Data). Commonly, bio-oil production from biomass via fast pyrolysis uses its own pyrolysis gas mixture (non-condensable gases) as fluidizing gas, where it needs to be sent back to the pyrolyzer (Peters et al., 2014; Jones et al., 2009; Wan Isahak et al., 2012). Therefore, the fluidizing gas, which is taken from the pyrolyzers' own gas output in the initial transient stages and then fully recycled at steady state, does not affect the net gas output of the pyrolyzer.

3.4. Furnace

Bio-char was separated from the condensable vapours and non-condensable gases released from the pyrolysis process using a cyclone and subsequently, the solid was combusted in a furnace alongside the non-condensable pyrolytic gases to provide heat for the pyrolyzer, as shown in Fig. 6. Heat integration then required 3% of the purified biomethane product to also be burnt to fully meet the pyrolyzer's heat duty. Combustion of the char required first an RYIELD block to artificially decompose the bio-char into its carbon, hydrogen, oxygen, and nitrogen constituents (Begum et al., 2013) based on the bio-char's ultimate analysis. This allowed an RGibbs block to represent the char combustion in the furnace under 20% excess of air, based on 1.10–1.30 air fraction range recommended for gas and pulverised coal combustion respectively (Jecht, 2004). CO_2, H_2O, CO and NO (S content neglected) were produced as flue gas. Further details of the heat duties met by the furnace are discussed in the 'Heat integration' section (3.7).

Downstream of the cyclone unit, the hot vapours after char separation were cooled down to 35 °C (Onarheim et al., 2014), which condensed the bio-oil into a liquid feed for the methanator unit, whereas the non-condensable gases were being burned. The phase change of bio-oil from vapour to liquid permits monitoring of the bio-oil yield and composition (moisture content, CHNS analysis), facilitating plant efficiency calculation and control, as well as optimisation measures at the pyrolysis stage, also enabling direct control of the S/C ratio in the methanator.

3.5. Methanation stage

There are several CO and CO_2 methanation processes that have been widely applied at industrial scale, such as Lurgi, TREMP, RMP and IRMA (Kopyscinski et al., 2010; Woodward, 1976; Hohlein et al., 1984). IRMA is the only methanation process that operates under isothermal conditions, while the rest (Lurgi, TREMP and RMP) operate in adiabatic conditions with intercooling stages. Since the methanation of CO is highly exothermic, at least two adiabatic reactors need to be implemented to run the methanation of CO process to ensure the feed gas will be nearly fully converted into methane. The direct methanation of PEFB-derived bio-oil is mildly exothermic, and therefore both adiabatic and isothermal methanators could be implemented, similarly to current designs of water gas shift reactors, without significant risk of hot spots (under adiabatic conditions) or cooling duty and control (under isothermal conditions). This is a major advantage of the new pyrolysis-direct methanation process compared to conventional gasification-methanation of CO in the thermochemical production of methane from lignocellulosic biomass.

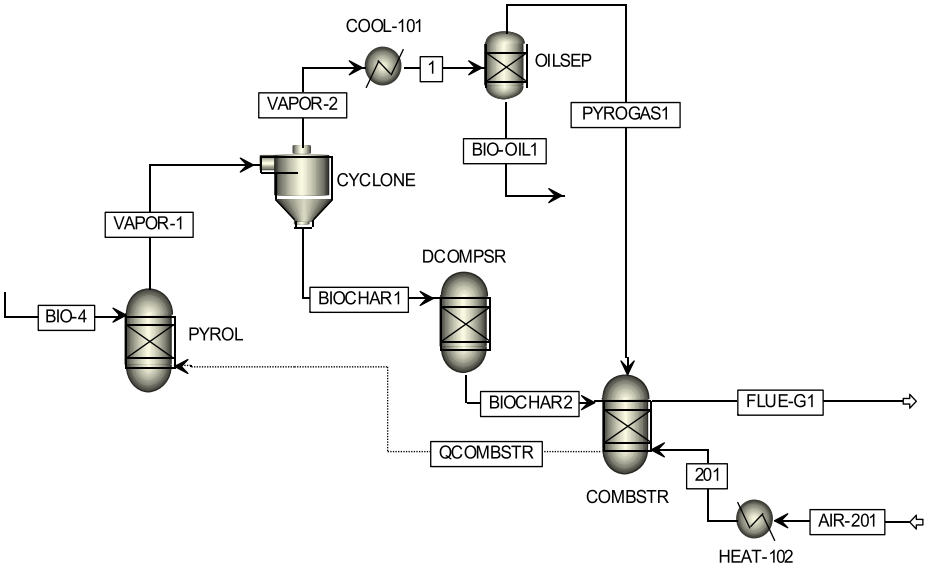

Fig. 6. Simplified flowsheet for the simulation of the PEFB fast pyrolysis process.

For simplicity, an isothermal reactor was selected (internally cooled reactor, type IRMA), as it is compatible with small to medium scale production plants (suitable for this case of study according to (Yun and Dupont, 2015)). The operating conditions for the isothermal methanator were 300 °C and 27 bar, and were selected based on industrial conditions of syngas conversion to methane (250–300 °C and 27–29 bar). Compared to the experiments, the lower temperature than 400 °C is afforded by compensating with operation at higher than atmospheric pressure, which would make the catalyst's kinetics and resulting activity equivalent. As prior to feeding the fixed bed catalytic LTSR methanator, the bio-oil from the pyrolysis process was pumped to 27 bar and then vaporized using flue gas heat recuperation before entering into the methanator, modelled as an 'RGibbs' block, as shown in Fig. 7. RGibbs reactors are modelled using the minimisation of Gibbs free energy method. Thus, the optimum condition to achieve the highest methane production was observed between S/C ratios of 2–3, resulting in 2198 kg/hr of water inlet needed in the feed corresponding to a S/C of 3. The simulation of the methanation plant revealed S/C ratios consistent with the AcOH experiments.

The gas output from the methanator (listed Table 4) is expectedly rich in CO_2 (45.1 mf mol %) as expressed in reaction EQ. 7. A first stage of purification of the biogas was implemented by dewatering via cooling down the stream to 25 °C. Then, the dry gas continuously flowed into a gas cleaning section, consisting of a high-pressure water scrubbing (HPWS) unit operating the CO_2 absorption at 25 bar.

3.6. Bio-SNG stream purification

A high-pressure water scrubbing (HPWS) system for biogas production from an anaerobic digestion process (Cozma et al., 2015) was used as a benchmark in this study to simulate the gas cleaning unit for upgrading CH_4 in the gas product stream. The conditions for the HPWS model in (Cozma et al., 2015) was based on data used in an existing commercial plant. Re-modelling the HPWS for bio-SNG production using the same operating parameters, which resulted in less than 5% error, allowed validating the model. Then, the parameters of the HPWS were adapted to maximize energy efficiency.

By operating the absorber column in the HPWS facility at 20 °C and 10 bar, it was determined that the solubility of CO_2 in water was 0.45 kg CO_2/100 kg water (Perkins and Innovates). Approximately 84,400 kg/h of total water was needed in order to absorb 380 kg/h of CO_2 in the crude biogas from the anaerobic process. However, it was assumed that 2.4% of the total water flow is lost due to evaporation (Cozma et al., 2015). Accordingly, at least 2000 kg/h of water is for make-up of losses, whereas 82,465 kg/h of water are part of the recycling closed loop (water pump around). Based on this work, almost 935 kg/h of CO_2 was produced from bio-oil conversion in the LTSR methanation process. By referring the operating conditions of the absorber column used in biogas production to those of an anaerobic digestion process (i.e. 20 °C and 10 bar), 187,000 kg of total water was required in HPWS unit, which corresponds approximately 0.50 kg CO_2/100 kg water of CO_2 (Perkins and Innovates). 4488 kg/h of water (i.e. 2.4% of the total water flow rate) were needed to replace the water lost due to the evaporation.

Table 4
Dry gas products from the methanation process (low purity bio-SNG). The conditions used in the methanator were an S/C of 3, 300 °C and 27 atm.

Dry gas products	Mol flowrate, kmol/h	mf mol%
Methane, CH_4	24.8	52.5
Carbon dioxide, CO_2	21.3	45.1
Carbon monoxide, CO	0.0	0.0
Hydrogen, H_2	1.1	2.4
Total	47.2	100.0

A pressure of 25 bar was selected to operate the absorber column of the HPWS unit. According to Henry's law, CO_2 dissolves in higher amounts in water at higher partial pressures. Some of the CH_4 product unfortunately also dissolves in the water flow alongside with CO_2. Separation of this gas-laden water was carried out in a flash drum at 3 bar, where the desorbed mixture of CH_4 and CO_2 gas was recycled with the fresh bio-methane after re-compression to 27 bar. The CO_2-laden water collected from the flash drum was then sent to the stripper for separate CO_2 and recycle water. Fig. 8 shows the flowsheet of HPWS which was used as a gas-cleaning unit.

The operating conditions of the HPWS unit used in this study and the compositions of upgraded gas products are listed in Table 5. A gas product with a composition of >99 wt % of CH_4 and <0.5 wt% of H_2 (corresponding to vol% of >95 and <5 respectively) and less than 4% of methane loss confirms the feasibility of the HPWS unit in this plant.

3.7. Heat integration

A minimum temperature difference, ΔT_{min} of 20 °C was used to ensure the driving force for the heat exchanger network. Table 6 lists stage 1 (air preheating by furnace flue gases), stages 2 and 3 (steam and bio-oil heat via recuperative heat), and stage 4 (superheating of both steam and bio-oil using furnace flue gases) as increasing levels of heat integration. Altogether, 25% of the biomethane product stream needed to be combusted in the central furnace to ensure the plant no longer relied on individual units's external heat inputs (Table 6), making it autothermal.

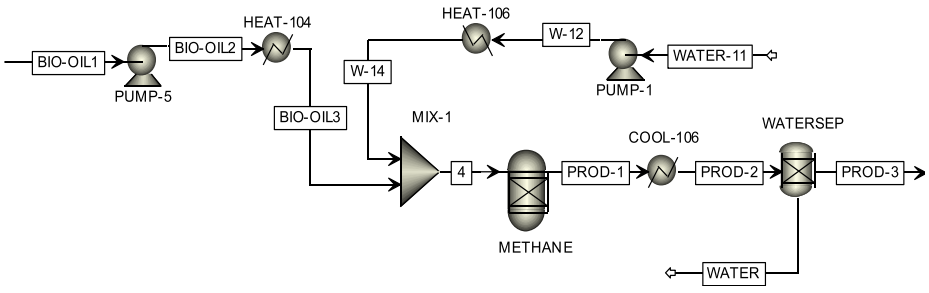

Fig. 7. Simulation flowsheet of the simplified methanation process.

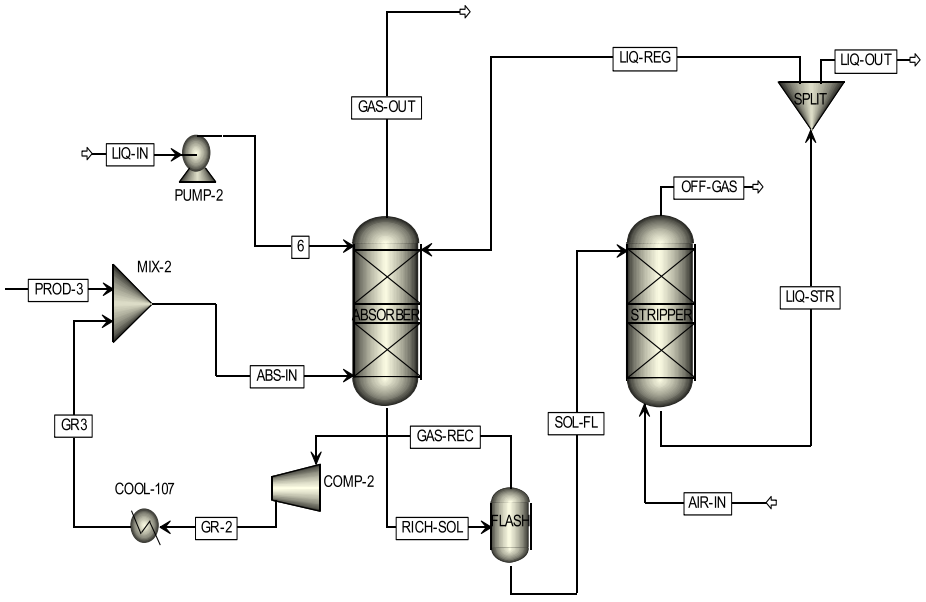

Fig. 8. Simulation flowsheet of the HPWS gas-cleaning system.

Table 5
Parameters values for HPWS simulation and compositions of the upgraded bio-methane production from PEFB bio-oil.

Parameters	Units	Parameters values
CH_4	kg/h	397.9
CO_2	kg/h	937.9
CO	kg/h	0.1
H_2	kg/h	2.3
$P_{absorber}$	bar	25
$P_{stripper}$	bar	1.0
$T_{absorber}$	°C	25
$T_{stripper}$	°C	25
Flowrate of gas feed (from methanator)	kg/h	1337.2
Water top-up	kg/h	4488
Air flow rate	kg/h	2859
Water-pump around	kg/h	182512
P_{flash}	bar	3
Number of theoretical stages		10
Upgraded bio-methane		
CH_4	kg/h (fraction of mass flowrate)	383.0 (0.994)
CO_2		0.0 (0.00)
CO		0.1 (0.00)
H_2		2.1 (0.006)
Treated flow rate	kg/h	385.2

3.8. Process performance

Different indicators such as energy conversion efficiency and energy consumption were determined, as well as compared with analogous processes of lignocellulosic biomass thermochemical conversion to biomethane such as biomass-to-fuel thermal efficiency (η_{btf}), as expressed in the expression EQ. 11, and the overall thermal efficiency (η_{th}) of the plant (EQ.12), takes into account the contributions of the electricity and heat net flows (Lind et al., 2012). Lower heating values (LHV) were used because the biomethane is intended to meet the immediate energy needs in the South East Asia and Sub-Saharan countries producers of PEFB.

$$\text{Biomass to fuel energy, } \eta_{btf} = \frac{\dot{m}_{methane} \times LHV_{methane}}{\dot{m}_{biomass} \times LHV_{biomass}} \quad \text{EQ. 11}$$

$$\text{Thermal efficiency, } \eta_{th} = \frac{\dot{m}_{methane} \times LHV_{methane} + (\dot{Q}^{-} - \dot{Q}^{+})}{\dot{m}_{biomass} \times LHV_{biomass} + (P_{el}^{+} - P_{el}^{-})} \quad \text{EQ. 12}$$

Fig. 9 shows the block diagram of the autothermal bio-methane plant (stage 4) and Fig. 10, which is an energy flows diagram, presents its energy use. The heat exported ($\dot{Q}^{-}$), power consumed or imported (P_{el}^{+}), and the balance between $\dot{m}_{biomass} \cdot LHV_{biomass}$ and $\dot{m}_{methane} \cdot LHV_{methane}$ values for the full integrated plant confirmed a significant improvement with respect of the non-integrated plant. In terms of performance, results of both configurations non-integrated and fully integrated, are shown in Table 7. Enhancement in thermal efficiency from the non-integrated plant (74.7% MW of bio-SNG/MW of biomass) to the autothermal plant (80.6%) was also revealed in Table 7, the latter compared favourably to the

Table 6
Heat and power of relevant process stages for integration stages: stage '1' = air preheat, '2' = partial steam generation+'1', '3' = partial bio-oil vaporisation+'2', '4' = complete steam and bio-oil superheating+'3'. (at stage 4, 25% product burns, plant is autothermal).

Energy demand, kW	w/o integration	Stage 1	Stage 2	Stage 3	Stage 4
Crushing	90				
Grinding	227				
Pump – Liquid bio-oil	3				
Pump – Water feed in methanation unit	6				
Compressor – Non-condensable pyrolysis gases	25				
HPWS power consumption	373				
Net power consumption ($P_{el}^{+}-P_{el}^{-}$)	**724**				
Cooling – After re-compression in HPWS unit	−430	−420	−430	−340	−430
Heating – Air for combustion	469	0	469	469	0
Heating-Drying wet PEFB	294	0	294	294	0
Cooling – After pyrolyzer	−662	−688	−641	−773	−344
Heating – Vaporized bio-oil	500	562	523	392	0
Heating – Vaporized water for methanation	1970	1970	925	1970	0
Methanation	−624	−726	0	−624	0
Cooling – After methanator	−2138	−2147	−1718	−2138	−1497
∑ of all excess heat rates ($\dot{Q}^{-}$)	3854	3981	2789	3875	2271
∑ of all heating demand rates ($\dot{Q}^{+}$)	3233	2532	2211	3125	0
Net excess heat rate ($\dot{Q}^{-}-\dot{Q}^{+}$)	**621**	**1449**	**578**	**750**	**2271**

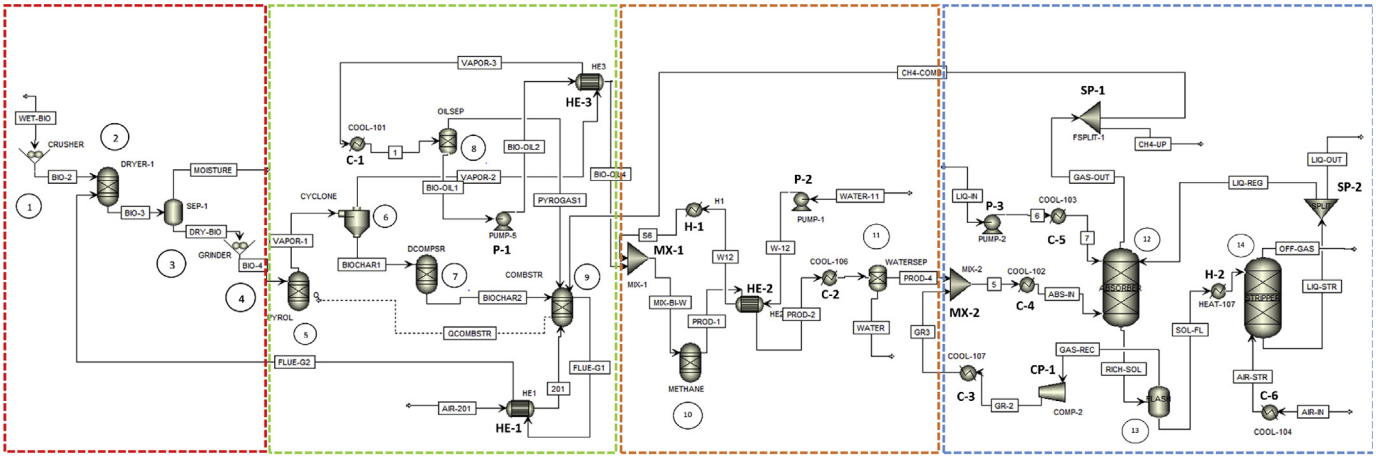

Biomass Pre-treatment		Pyrolysis		Methanation		HPWS	
1	Biomass crusher	5	Pyrolyser (RYIELD)	10	Isothermal methanator (RGIBBS)	12	Absorber
2	Rotary dryer (RYIELD)	6	Cyclone	11	Water separator	13	Stripper
3	Separator	7	Bio-char decomposer (RYELD)			14	Flash drum
4	Grinder	8	Bio-oil separator				
		9	Furnace (RGIBBS)				
C-1 to C-6				Coolers			
H-1 and H-2				Heaters			
P-1 to P-3				Pumps			
HE-1 to HE-3				Heat exchangers			
CP-1				Compressor			
MX-1 to MX-2 and SP-1 to SP-2				Stream mixer and splitter			

Fig. 9. Aspen plus simulation flowsheet with air-preheat, steam and bio-oil vaporisation integration: results for methanation plant with configuration 4 *(see separate Fig. 9 file).*

range from the literature 71.2–91.0% (Table 8 whose inputs are detailed in supplementary data).

Other performance indicators are introduced in Table 8 (all workings shown in supplementary data) to account for the different quality of feedstock across the literature on gasification-methanation, one of them is the percentage of efficiency of methane yield, defined as the ratio of the plant-derived methane yield to that of the maximum stoichiometric methane yield achievable by complete conversion of the biomass source to methane according to (EQ. 7). This indicator allows comparing different gasification plants performance despite their operation with diverse biomass feedstocks.

Overall carbon conversion efficiency (Duret et al., 2005),

$$\eta_C = \frac{\dot{n}_{C,out}}{\dot{n}_{C,in}} \qquad \text{EQ. 13}$$

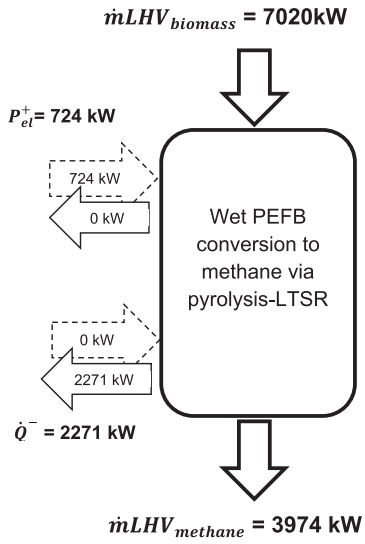

Fig. 10. Energy flow diagram in the methanation plant via pyrolysis-LTSR (heat integrated, process 4).

Based on results listed in Table 8, which were calculated from the stoichiometry of the methanation of the biomass reaction (EQ. 7), the maximum theoretical CH_4 yield when using PEFB feed was 36.1 wt% compared to that from wood (32.2–35.0 wt%) for CH_4 production. In addition, the efficiencies of CH_4 production compared to the maximum of theoretical CH_4 production for PEFB were 53.2–70.8%, which were within the range of the wood gasification process (63.6–80.6%). The overall carbon conversion efficiency (listed in Table 8) for the non-integrated and stage 4-autothermal plant were calculated to be 39.1% and 30.5%, respectively, compared to 32.0–42.5% for wood gasification.

4. Conclusion

Acetic acid (as single compound bio-oil surrogate) conversion to CH_4 using a Ni/Ca–Al_2O_3 catalyst was feasible by direct methanation via the low temperature steam reforming (LTSR) process. At (9.5×10^{-6} mol_C/s) feed, the highest CH_4 yield was 15.7 wt% of the feed, at 400 °C and feed molar S/C ratio of 2. A plant design for the production of high purity biomethane from very moist PEFB was subsequently presented, which included drying, chopping, fast pyrolysis, direct methanation of the bio-oil, and CO_2 removal by high-pressure water scrubbing. Burning 25% of the upgraded biomethane product in addition to the bio-char and the non-condensable gases from the pyrolysis were required for autothermal operation. The estimated thermal efficiencies increased from 74.7% (MW of bio-SNG/MW of biomass) for the allothermal plant to 80.6% (MW of bio-SNG/MW of biomass) for the autothermal plant. These were comparable with the-state-of-art biomass gasification route to methane production via syngas followed by CO and CO_2 methanation, although avoiding the generation of heavy tars and the large temperature swings between units. It is therefore expected that capital and operational expenditures of the pyrolysis-direct methanation of bio-oil will be lower when operating using similar lignocellulosic biomass feedstock recalcitrant to bio-processing. Practical challenges arise from avoiding carbon accumulation on the catalyst during the direct methanation of bio-oil, which will be explored in future works.

Table 7
Comparison of the performance between plant designs without heat integration and with integration stage 4.

Parameters	w/o integration: Plant relies on local external heat inputs	Integration stage 4: Plant operates w/o external heat inputs
$LHV_{PEFB(wet)}$, kWh/kg	2.34	
$LHV_{methane}$, kWh/kg	13.8	
Mass flow rate of raw PEFB, kg/h	3000	
Mass flow rate of pure CH_4 production, kg/h	370	288
Net power consumption (P_{el}^{+} - P_{el}^{-}), kW	640	724
Net excess heat ($Q^{-} + Q^{+}$), kW	621	2271
η_{btf}, % (kW of CH_4/kW of biomass)	72.7	56.6
η_{th}, % (kW of CH_4/kW of biomass)	74.7	80.6

Table 8
Process performance of this work compared to the literature. See Table 3 for elemental analyses of each biomass and LHV_{dry}. This work: (a) w/o (b) w/integration stage 4.

Biomass	This work		Fendt et al. (2012)	Tremel et al. (2013)	Van der Meijden et al. (2010)	Gassner and Maréchal (2009)	Duret et al. (2005)
	(a)PEFB	(b)PEFB	Beech	Spruce	Wood	Wood	Wood
$C_nH_mO_k$	$CH_{1.57}O_{0.59}$	$CH_{1.57}O_{0.59}$	$CH_{1.43}O_{0.71}$	$CH_{1.50}O_{0.65}$	$CH_{1.43}O_{0.63}$	$CH_{1.34}O_{0.63}$	$CH_{1.57}O_{0.73}$
$LHV_{biomass,wet}$ (MJ)	8.42	8.42	13.23	14.55	15.98	9.30	18.20
CH_4 yield wt.% of dry biomass (Aspen plus model)	24.7	19.2	20.5	28.2	n/a	27.4	21.2
Maximum theoretical CH_4 yield, wt.% of dry biomass	36.1	36.1	32.2	35.0	34.9	34.5	32.5
% efficiency of CH_4 (Aspen plus/max theor yield. CH_4)	70.8	53.2	63.6	80.6	n/a	79.5	65.1
η_{btf}, % (MJ of max theor. CH_4/MJ of biomass) (R-11)	106.9	106.9	97.0	89.9	n/a	92.5	89.1
η_{btf}, % (MJ of CH_4/MJ of biomass, Aspen Plus)	72.7	56.7	61.8	72.5	n/a	73.5	58.0
η_{btf}, % (MJ of bio-SNG/MJ of biomass, Aspen Plus)	72.7	57.1	62.5	73.7	70.3	73.8	n/a
η_{th}, % (MW of bio-SNG/MW of biomass) (R-12)	74.7	80.6	71.2	91.0	n/a	n/a	n/a
η_C, % (kmol.s^{-1} CH_4 prod/kmol.s^{-1} of inlet C) (R-13)	39.1	30.5	32.0	42.5	n/a	40.6	33.5

Acknowledgments

The following are acknowledged: The Ministry of Education of Malaysia (EM) for financial support in the form of the PhD scholarship of Dr Hafizah Abdul Halim Yun; CONACYT (México) for the financial support in the form of the PhD scholarship of Dr Sergio Ramírez Solís; Dr Martyn V. Twigg at TST Limited, UK, for in-kind support in the form of the NiO/Calcium Aluminate catalyst; and to EPSRC via grants EP/K000446/1 (UKCCSRC grant call 2, C2-181) and EP/R030243/1 (EPSRC GCRF Creating Resilient Sustainable Microgrids through Hybrid Renewable Energy Systems CRESUM-HYRES), which allowed purchase and use of the research licenses of Aspen Plus V8.8 (early work) and V10 (later work).

Appendix A. Supplementary data

Supplementary data to this article can be found online at https://doi.org/10.1016/j.jclepro.2019.118737

References

Abas, R., Kamaruddin, M.F., Nordin, A.B.A., Simeh, M., 2011. A study on the Malaysian oil palm biomass sector—supply and perception of palm oil millers. Oil Palm Industry Economic Journal 11 (1), 28–41.
Abdullah, N., Gerhauser, H., Bridgwater, A.V., 2007. Bio-oil from fast pyrolysis of oil palm empty fruit bunches. J. Phys. Sci. 1 (1), 57–74.
Abdullah, N., Sulaiman, F., Gerhauser, H., 2011. Characterisation of oil palm empty fruit bunches for fuel application. J. Phys. Sci. 22 (1), 1–24.
Abu Bakar, W.A.W., Ali, R., Toemen, S., 2011. Catalytic methanation reaction over supported nickel-rhodium oxide for purification of simulated natural gas. J. Nat. Gas Chem. 20 (6), 585–594.
Amos, W.A., 1998. Report on Biomass Drying Technology. Midwest Research Institute, Colorado, U.S.
Begum, S., Rasul, M.G., Akbar, D., Ramzan, N., 2013. Performance analysis of an integrated fixed bed gasifier model for different biomass feedstocks. Energies 6 (12), 6508–6524.
Bridgwater, A.V., 2012. Review of fast pyrolysis of biomass and product upgrading. Biomass Bioenergy 38, 68–94.
Channiwala, S.A., Parikh, P.P., 2002. A unified correlation for estimating HHV of solid, liquid and gaseous fuels. Fuel 81 (8), 1051–1063.
Cozma, P., Wukovits, W., Mămăligă, I., Friedl, A., Gavrilescu, M., 2015. Modeling and simulation of high pressure water scrubbing technology applied for biogas upgrading. Clean Technol. Environ. Policy 17 (2), 373–391.
Dincer, I., Acar, C., 2015. Review and evaluation of hydrogen production methods for better sustainability. Int. J. Hydrogen Energy 40 (34), 11094–11111.
Dudley, B.J.L., UK, 2016. BP Statistical Review of World Energy, 2015.
Duret, A., Friedli, C., Maréchal, F., 2005. Process design of Synthetic Natural Gas (SNG) production using wood gasification. J. Clean. Prod. 13 (15), 1434–1446.
Fagernäs, L., Brammer, J., Wilén, C., Lauer, M., Verhoeff, F., 2010. Drying of biomass for second generation synfuel production. Biomass Bioenergy 34 (9), 1267–1277.
Fendt, S., Tremel, A., Gaderer, M., Spliethoff, H., 2012. The potential of small-scale SNG production from biomass gasification. Biomass Conversion and Biorefinery 2 (3), 275–283.
Gao, J.J., Jia, C.M., Zhang, M.J., Gu, F.N., Xu, G.W., Su, F.B., 2013. Effect of nickel nanoparticle size in Ni/alpha-Al2O3 on CO methanation reaction for the production of synthetic natural gas. Catalysis Science & Technology 3 (8), 2009–2015.
Garbarino, G., Riani, P., Magistri, L., Busca, G., 2014. A study of the methanation of carbon dioxide on Ni/Al2O3 catalysts at atmospheric pressure. Int. J. Hydrogen Energy 39 (22), 11557–11565.
Garcia-Perez, M., Chaala, A., Pakdel, H., Kretschmer, D., Roy, C.J.B., Bioenergy, 2007. Characterization of bio-oils in chemical families, 31 (4), 222–242.
Gassner, M., Maréchal, F., 2009. Thermo-economic process model for thermochemical production of Synthetic Natural Gas (SNG) from lignocellulosic biomass. Biomass Bioenergy 33 (11), 1587–1604.
Göransson, K., Söderlind, U., He, J., Zhang, W., 2011. Review of syngas production via biomass DFBGs. Renew. Sustain. Energy Rev. 15 (1), 482–492.
Hohlein, B., Niessen, H., Range, J., Schiebahn, H.J.R., Vorwerk, M., 1984. Methane from synthesis gas and operation of high-temperature methanation. Nucl. Eng. Des. 78 (2), 241–250.
Jecht, U., 2004. Flue Gas Analysis in Industry: Practical Guide for Emission and Process Measurements (testo).
Jones, S.B., Valkenburg, C., Walton, C.W., Elliott, D.C., Holladay, J.E., Stevens, D.J., Kinchin, C., Czernik, S., 2009. Production of Gasoline and Diesel from Biomass via Fast Pyrolysis, Hydrotreating and Hydrocracking: a Design Case. Pacific Northwest National Laboratory, Richland, WA.
Kerdsuwan, S., Laohalidanond, K., 2011. Renewable Energy from Palm Oil Empty Fruit Bunch. INTECH Open Access Publisher.
Kopyscinski, J., Schildhauer, T.J., Biollaz, S.M.A., 2010. Production of synthetic natural gas (SNG) from coal and dry biomass - a technology review from 1950 to 2009. Fuel 89 (8), 1763–1783.
Li, J., Zhou, L., Li, P.C., Zhu, Q.S., Gao, J.J., Gu, F.N., Su, F.B., 2013. Enhanced fluidized bed methanation over a Ni/Al2O3 catalyst for production of synthetic natural gas. Chem. Eng. J. 219, 183–189.
Lind, F., Heyne, S., Johnsson, F., 2012. What Is the Efficiency of a Biorefinery?.
Machinery, A., 12 May 2016. *Supply EFB (empty palm fruit bunch) pellet production line*. 12 january *2015*. Available from: https://www.linkedin.com/pulse/supply-efb-empty-palm-fruit-bunch-pellet-production-line-bella-wu.
Mohammed, M.A.A., Salmiaton, A., Wan Azlina, W.A.K.G., Mohamad Amran, M.S., 2012. Gasification of oil palm empty fruit bunches: a characterization and kinetic study. Bioresour. Technol. 110, 628–636.
Ni, M., Leung, D.Y.C., Leung, M.K.H., Sumathy, K., 2006. An overview of hydrogen production from biomass. Fuel Process. Technol. 87 (5), 461–472.
Onarheim, K., Solantausta, Y., Lehto, J., 2014. Process simulation development of fast pyrolysis of wood using aspen plus. Energy Fuels 29 (1), 205–217.
Owusu, P.A., Asumadu-Sarkodie, S., 2016. A review of renewable energy sources, sustainability issues and climate change mitigation. Cogent Engineering 3 (1), 1167990.
Perkins, E. and A. Innovates, Fundamental Geochemical Processes between CO2, Water and Minerals. Alberta Innovates–Technology Futures.
Peters, J.F., Petrakopoulou, F., Dufour, J., 2014. Exergetic analysis of a fast pyrolysis process for bio-oil production. Fuel Process. Technol. 119, 245–255.
Phillips, S., Aden, A., Jechura, J., Dayton, D., Eggeman, T., 2007. Thermochemical Ethanol via Indirect Gasification and Mixed Alcohol Synthesis of Lignocellulosic Biomass. National Renewable Energy Lab.(NREL), Golden, CO (United States).
Pimenidou, P., Dupont, V., 2012. Characterisation of palm empty fruit bunch (PEFB) and pinewood bio-oils and kinetics of their thermal degradation. Bioresour. Technol. 109, 198–205.
Ruengvilairat, P., Tanatavikorn, H., Vitidsant, T., 2012. Bio-oil production by pyrolysis of oil palm empty fruit bunch in nitrogen and steam atmospheres. J. Sustain. Bioenergy Syst. 2 (4), 75.
Shariff, A., Mohamad Aziz, N.S., Abdullah, N., 2014. Slow pyrolysis of oil palm empty fruit bunches for biochar production and characterisation. J. Phys. Sci. 25 (2), 97.
Sharma, A., Shinde, Y., Pareek, V., Zhang, D., 2015. Process modelling of biomass conversion to biofuels with combined heat and power. Bioresour. Technol. 198, 309–315.
Singh, P., Bajpai, U., 2012. Anaerobic digestion of flower waste for methane production: an alternative energy source. Environ. Prog. Sustain. Energy 31 (4), 637–641.
Solarte-Toro, J.C., Chacón-Pérez, Y., Cardona-Alzate, C.A., 2018. Evaluation of biogas and syngas as energy vectors for heat and power generation using lignocellulosic biomass as raw material. Electron. J. Biotechnol. 33, 52–62.
Sukiran, M.A., Chin, C.M., Bakar, N.K., 2009. Bio-oils from pyrolysis of oil palm empty fruit bunches. Am. J. Appl. Sci. 6 (5), 869–875.
Sukiran, M.A., Kheang, L.S., Bakar, N.A., May, C.Y., 2011. Production and characterization of bio-char from the pyrolysis of empty fruit bunches. Am. J. Appl. Sci. 8 (10), 984.
Thunman, H. and M. Seemann. Advanced insintric syngas cleaning and increased bioSNG efficiency. in *REGATEC 2017*. 2017. Pacengo (Verona), Italy: Renewable Energy Technology International AB.
Tremel, A., Gaderer, M., Spliethoff, H., 2013. Small-scale production of synthetic natural gas by allothermal biomass gasification. Int. J. Energy Res. 37 (11), 1318–1330.
Van der Meijden, C.M., Veringa, H.J., Rabou, L.P.L.M., 2010. The production of synthetic natural gas (SNG): a comparison of three wood gasification systems for energy balance and overall efficiency. Biomass Bioenergy 34 (3), 302–311.
Vitasari, C.R., Jurascik, M., Ptasinski, K.J., 2011. Exergy analysis of biomass-to-synthetic natural gas (SNG) process via indirect gasification of various biomass feedstock. Energy 36 (6), 3825–3837.
Wan Isahak, W.N.R., Hisham, M.W.M., Yarmo, M.A., Hin, T.-y.Y., 2012. A review on bio-oil production from biomass by using pyrolysis method. Renew. Sustain. Energy Rev. 16 (8), 5910–5923.
Ward, J., Rasul, M.G., Bhuiya, M.M.K., 2014. Energy recovery from biomass by fast pyrolysis. Procedia Engineering 90, 669–674.
White, R., Dupont, V., Cockerill, T., 2018. Thermodynamic modelling and energy balance of direct methanation of glycerol for Bio-SNG production. Energy Convers. Manag. 160, 354–363.
Woodward, C., 1976. High-temperature methanation catalyst for SNG applications. Am. Chem. Soc., Div. Fuel Chem., Prepr.;(United States) 21 (4).
Yang, H., Yan, R., Chen, H., Lee, D.H., Liang, D.T., Zheng, C., 2006. Pyrolysis of palm oil wastes for enhanced production of hydrogen rich gases. Fuel Process. Technol. 87 (10), 935–942.
Yun, H.A.H., Dupont, V., 2015. Thermodynamic analysis of methanation of palm empty fruit bunch (PEFB) pyrolysis oil with and without in situ CO2 sorption. AIMS Energy 3 (4), 774–797.
Zhang, R., Cummer, K., Suby, A., Brown, R.C., 2005. Biomass-derived hydrogen from an air-blown gasifier. Fuel Process. Technol. 86 (8), 861–874.
Zhang, W., He, J., Engstrand, P., Björkqvist, O., 2015. Economic evaluation on bio-synthetic natural gas production integrated in a thermomechanical pulp mill. Energies 8 (11), 12795–12809.
Zin, R.M., Lea-Langton, A., Dupont, V., Twigg, M.V., 2012. High hydrogen yield and purity from palm empty fruit bunch and pine pyrolysis oils. Int. J. Hydrogen Energy 37 (14), 10627–10638.